Title:

Towards a universal model for carbon dioxide uptake by plants

Authors:

Han Wang[1,2,3*], I. Colin Prentice[1,2,4], Trevor F. Keenan[2,5], Tyler W. Davis[4,6], Ian J. Wright[2] , William K. Cornwell[7], Bradley J. Evans[2,8] and Changhui Peng[1,9*]

Affiliations:

[1] State Key Laboratory of Soil Erosion and Dryland Farming on the Loess Plateau, College of Forestry, Northwest A & F University, Yangling 712100, Shaanxi, China

[2] Department of Biological Sciences, Macquarie University, North Ryde, NSW 2109, Australia

[3] Ecosystems Services and Management Program, International Institute for Applied Systems Analysis, Laxenburg, A-2361, Austria

[4] AXA Chair of Biosphere and Climate Impacts, Department of Life Sciences, Imperial College London, Silwood Park Campus, Buckhurst Road, Ascot SL5 7PY, UK

[5] Earth Sciences Division, Lawrence Berkeley National Laboratory, 1 Cyclotron Road, Berkeley, CA 94720, United States

[6] United States Department of Agriculture-Agricultural Research Service, Robert W. Holley Center for Agriculture and Health, Ithaca, NY 14853, United States

[7] Ecology and Evolution Research Centre, School of Biological, Earth and Environmental Sciences, The University of New South Wales, Randwick, NSW 2052, Australia

[8] Faculty of Agriculture and Environment, Department of Environmental Sciences, The University of Sydney, NSW 2006, Australia

[9] Department of Biological Sciences, Institute of Environmental Sciences, University of Quebec at Montreal, C.P. 8888, Succ. Centre-Ville, Montréal H3C 3P8, Québec, Canada

Manuscript type: Letter

[*]Correspondence to:

H Wang: wanghan_sci@yahoo.com, C Peng: peng.changhui@uqam.ca

Introductory paragraph

Gross primary production (GPP) – the uptake of CO_2 by leaves, and its conversion to sugars by photosynthesis – is the basis for life on land. Earth System Models (ESMs) incorporating the interactions of land ecosystems and climate are used to predict the future of the terrestrial sink for anthropogenic carbon dioxide (CO_2)[1]. ESMs require accurate representation of GPP. But current ESMs disagree on how GPP responds to environmental variations[1,2], suggesting a need for a more robust theoretical framework for modelling[3,4]. Here we focus on a key quantity for GPP, the ratio of leaf-internal to external CO_2 (χ). χ is tightly regulated and depends on environmental conditions, but is represented empirically and incompletely in today's models. We show that a simple evolutionary optimality hypothesis[5,6] predicts specific quantitative dependencies of χ on temperature, vapour pressure deficit and elevation; and that these same dependencies emerge from an independent analysis of empirical χ values, derived from a worldwide data set of > 3500 leaf stable carbon isotope measurements. A single global equation embodying these relationships then unifies the empirical light use efficiency (LUE) model[7] with the standard model of C_3 photosynthesis[8], and successfully predicts GPP measured at eddy-covariance flux sites. This success is notable given the equation's simplicity and broad applicability across biomes and plant functional types. It provides a theoretical underpinning for the analysis of plant functional co-ordination across species and emergent properties of ecosystems, and a potential basis for the reformulation of the controls of GPP in next-generation ESMs.

The standard model[8] accurately describes the instantaneous environmental and physiological controls of photosynthesis, whereas empirical LUE models can predict primary production over weeks to months[7,9] (Supplementary Information). The connection between these parallel modelling frameworks remains unresolved[9]. Both require independent information to be provided: leaf-internal CO_2 partial pressure (c_i) and photosynthetic capacities for carboxylation and electron transport (V_{cmax} and J_{max}) in the Farquhar model, and environmental response functions in LUE models. There is no accepted general way to do this for large-scale modelling[10,11], and as a result, different implementations of apparently the same model can give very different answers in different ESMs.

The biochemical reactions of photosynthesis depend on the value of c_i[8,12]. CO_2 diffuses into leaves through the stomata (microscopic pores in the leaf surface) towards the chloroplasts, where reducing power derived from solar energy is used to assimilate CO_2 into organic forms through the Calvin cycle. The term c_i refers to the partial pressure of CO_2 in the intercellular space, which is lower than the ambient CO_2 partial pressure (c_a) while photosynthesis is active due to the resistance imposed by the stomata. The term c_c (applying at the chloroplasts, where carbon fixation occurs) is generally even smaller than c_i due to additional resistance to CO_2 transport in the mesophyll (a point that we return to later) but most current models disregard this additional drawdown of CO_2. Thus, given knowledge of c_a, the quantity $\chi = c_i/c_a$ becomes a key modelling target. χ is tightly regulated by the fast (time scale of minutes) responses of both photosynthetic rate and stomatal aperture to environmental fluctuations. However, current stomatal models used in ESMs account only for the response of χ to

moisture, represented by empirical and non-equivalent formulations[13]; while satellite-based products based on LUE do not represent c_i at all (Supplementary Information). We propose that a firm basis for the prediction of χ is an essential first step towards a first-principles representation of terrestrial plant carbon uptake.

Long-term effective values of χ can be reconstructed from data on leaf stable carbon isotope ratios ($\delta^{13}C$). Previous analyses of leaf $\delta^{13}C$ data have examined relationships with environmental factors statistically, with many using leaf $\delta^{13}C$ as a palaeoclimatic indicator of moisture-related climate variables only[14]. Here we predict the environmental responses of χ theoretically, reserving the leaf $\delta^{13}C$ measurements for testing. Our theoretical approach depends on the idea of evolutionary optimality in balancing the costs of water loss and carbon gain – a long-standing source of hypotheses to account for stomatal behavior[15,16]. We derive theoretical dependencies of 'optimal' χ (termed χ_o) on growing-season air temperature, vapour pressure deficit, and elevation above sea level based on the least-cost hypothesis[5,6], which states that plants minimize the combined costs of maintaining the capacities for carboxylation (maintaining the activity of Rubisco, the primary carboxylating enzyme, and other photosynthetic proteins) and transpiration (maintaining living tissues to support water transport) required to achieve a given assimilation rate. We derive effective growing-season values of χ from a large global compilation of $\delta^{13}C$ measurements on leaves of C_3 plants[17] (Supplementary Figure 1) with a standard method[18], and use these values to test the theory's predictions. We then invoke the hypothesis of co-limitation between carboxylation- and electron transport-limited photosynthetic rates to provide a universal model of GPP in C_3 plants, which is shown to unify the Farquhar and LUE models for C_3 photosynthesis. Finally the model is tested against GPP data derived from eddy-covariance flux measurements.

The theory developed in Methods predicts that the quantity logit (χ_o) = ln [χ_o / (1 – χ_o)] should rise with growth temperature (T_g) by ~ 0.0545 per Kelvin due to increased assimilation costs (the affinity of Rubisco for CO_2 *versus* O_2 declines with temperature) and reduced water transport costs (the viscosity of water declines). Due to the increase in transpiration costs imposed by increasing vapour pressure deficit (vpd), logit (χ_o) also should fall by 0.5 per unit increase of natural log transformed D_0 (the vpd that would be obtained at standard atmospheric pressure under the same temperature and H_2O mole fraction). With increasing elevation the saturated vapour pressure of water remains constant while the actual vapour pressure (all other factors constant) declines, implying increased transpiration costs; while the partial pressure of O_2 also declines, increasing the affinity of Rubisco for CO_2 and implying reduced assimilation costs[19]. These two effects combine to yield a reduction of logit (χ_o) by ~ 0.0815 per km elevation (z). The theoretical model for χ_o can therefore be written in a linearized form:

$$\ln [\chi_o/(1-\chi_o)] \approx 0.0545\,(T_g - 25) - 0.5 \ln D_0 - 0.0815\,z + C \qquad (1)$$

These predicted effects of each variable are shown here to be quantitatively consistent with the corresponding partial effects (that is, effects of each variable with the others held constant) independently inferred from the leaf χ data by multiple regression (Fig. 1, Table 1). Fitting this equation (with fixed coefficients) to the data provided an estimate of C = 1.189, close to the value of

1.168 obtained with variable coefficients (Table 1). This constant is directly related to β, the ratio of carboxylation to transpiration cost factors at 25˚C, by equation (12) in Methods. The coefficients in equation (1) were computed for standard conditions (T_g = 25 ˚C, D_0 = 1 kPa, z = 0 km). The coefficient for elevation is sensitive to relative humidity (RH) at standard pressure, however, and becomes arbitrarily large as RH approaches 100%. The value of –0.0815 was computed at RH = 50%. As predicted, the fitted (negative) slope of ln [χ / (1 – χ)] with elevation increases with RH, most steeply at high RH (Fig. 1).

χ_o values from equation (1) are consistent with observed χ across biomes (r = 0.51) (Fig. 2). Highest values are in hot, wet, low-elevation sites (tropical forests), lowest in cold and/or dry and/or high-elevation sites (deserts, polar and alpine vegetation). χ_o ranges globally from 0.4 to almost 1.0 with a typical value of 0.77 (Supplementary Figure 2). The reduction from the equator towards mid-latitudes is due to increasing aridity while that in high latitudes is due to declining temperatures (Supplementary Figure 3).

Using a published dataset of CO_2 and water exchange measurements[20], we confirmed (Supplementary Table 1) that the partial effects of temperature and vpd on instantaneous gas exchange are also consistent with equation (1). No elevation effect was found, however, probably due to the limited elevation range in this dataset.

So far, we have implicitly assumed infinite mesophyll conductance and, therefore, that the ratio (χ_c) of CO_2 partial pressure at the chloroplasts (c_c) to c_a equals the ratio of c_i to c_a. In Methods we show that the optimal value of χ_c has the same environmental dependencies as χ_o, with an additional dependency on the ratio of g_s to g_m. Values of χ_c were estimated from the leaf data using a process-based model for ^{13}C discrimination. Data analysis confirmed the predicted environmental responses of logit (χ_c), but with a lower estimate of C = 1.097 (Supplementary Table 2) as expected, since finite g_m implies $\chi_c < \chi$. The agreement between observed and predicted χ_c was slightly improved compared to that of χ (Supplementary Table 2, Supplementary Figure 4).

The co-ordination or co-limitation hypothesis, stating that the two photosynthetic processes of carboxylation and transport are coupled such that photosynthetic rates limited by those two processes are equal under typical daytime conditions, provides the next step towards a universal model of GPP[21,22]. The hypothesis implies adjustment of V_{cmax} in time and space to match environmental conditions[22] and predicts environmental responses of GPP in the field that are necessarily different from those observed in laboratory experiments which are typically conducted at light saturation, with no time for acclimation. Extensive field measurements also point to an optimal maximum rate of electron transport, J_{max}, that maximizes the photosynthetic benefits minus the costs of maintaining the electron-transport chain (Supplementary Figure 5)[23]. We can thereby eliminate both V_{cmax} and J_{max} as independent predictors, to derive a first-principles model for C_3 photosynthesis on weekly or longer time scales that has the mathematical form of a LUE model, but is nonetheless consistent with the standard model of C_3 photosynthesis:

$$\mathrm{GPP} = \varphi_0 I_{abs} m \sqrt{[1 - (c^*/m)^{2/3}]} \quad (2)$$

where

$$m = (c_a - \Gamma^*)/\{c_a + 2\Gamma^* + 3\Gamma^*\sqrt{[1.6\,\eta^* D_0 \beta^{-1} (K + \Gamma^*)^{-1}]}\} \quad (3)$$

Here φ_0 is the intrinsic quantum yield (1.02 g C mol^{-1})[24], I_{abs} is the absorbed photosynthetic photon flux density (PPFD, mol m^{-2} s^{-1}), Γ^* is the photorespiratory compensation point (Pa), K is the effective Michaelis-Menten coefficient of Rubisco (Pa), η^* is the viscosity of water relative to its value at 25°C, $\beta \approx 240$ from the constant C in equation (1), and c^* is proportional to the unit carbon cost for the maintenance of electron transport capacity, ≈ 0.41 (estimated from observed J_{max}:V_{cmax} ratios). Although not explored here, GPP of C_4 plants under field conditions can be represented using a modification of equations (2) and (3), given that C_4 plants boost CO_2 around the chloroplasts to high levels while operating at a lower φ_0.

For C_3 plants, the LUE is the product of φ_0, m and the square-root term in equation (2). Thus GPP is proportional to I_{abs}, which can be calculated as the product of incident PPFD and remotely sensed green vegetation cover. LUE is less than the potential maximum (φ_0) due to limitations by CO_2 (m) and electron transport capacity (the square-root term) leading to global mean reductions by 25% and 43%, respectively. Supplementary Figure 6 shows how the predicted global pattern of potential maximum GPP by C_3 plants is modified by those constraints.

Predicted monthly GPP compares well with monthly GPP derived from CO_2 flux measurements (Fig. 3). Predicted global total annual GPP is 120 Pg C, within the accepted range[25]. The model captures the variation in observed GPP within and among different biomes as well as or better than other LUE models[26] (Supplementary Information, Supplementary Table 3). This level of predictability, achieved with only two free parameters (β and c^*) that are estimated from independent observations, suggests that variations in χ and LUE that are commonly represented by biome-specific parameters could be explained more parsimoniously as a consequence of optimal plant responses to the climates in which different biomes occur.

Enhanced LUE and GPP are predicted with increasing c_a, the magnitude of the enhancement varying with climate. A meta-analysis of 12 Free Air Carbon dioxide Enrichment experiments showed that with CO_2 increased by about 200 ppm, LUE and instantaneous water use efficiency increased by 12.2 ± 9% and 54.3 ± 17%, while the ratio V_{cmax}/J_{max} and stomatal conductance changed by –4.9 ± 2.8% and –20 ± 3%[27]. The model-predicted mean changes in these quantities in turn (Supplementary Information) are 17.2%, 55%, –22.4% and –15%. This analysis also showed a slight (non-significant) CO_2-induced reduction in χ, consistent with the prediction of a slight decline by equation (9). Considering finite g_m slightly enhances the LUE increase and reduces V_{cmax}/J_{max} decrease due to CO_2 enrichment but has no effect on the responses of water use efficiency and g_s. The model's overestimation of the CO_2 effect on V_{cmax}/J_{max} requires further analysis: for example we note that increased leaf temperature due to stomatal closure under CO_2 enrichment would impose a strong positive effect on V_{cmax}/J_{max} (~ 4% per K), potentially compensating the CO_2 effect.

Consideration of finite g_m (substituting χ_c for χ_o) affects the interpretation of β, which is reduced to ≈ 200 and now incorporates both the ratio of cost factors and the ratio of g_s to g_m. This modification reduces global annual GPP by 2.5% and marginally improves the agreement with observations (r = 0.742, RMSE = 68.69 g C month^{-1}).

The spread of χ and GPP values around the model predictions may reflect variation in β and c^* which have so far been assumed constant. It will be worthwhile to explore their possible dependencies on plant functional traits. For example, the unit cost of transpiration is expected to depend on plant hydraulic traits, including the density and permeability of conducting tissue, plant height and the isohydry-anisohydry continuum, which together with soil moisture determines the maximum water potential difference between soil and leaf[5]. We found no significant difference in χ between woody and non-woody plants; the differences in ^{13}C discrimination among conventionally defined plant functional types (PFTs) were predicted correctly by climate and elevation alone (Supplementary Figure 7). Nonetheless, we did find a significant difference between gymnosperms and angiosperms (20% higher water cost in gymnosperms suggested by the global carbon isotope dataset: Supplementary Information) which could be explained by the narrower conducting elements of gymnosperms, and is consistent with the observed high intrinsic water use efficiency of conifer forests[28]. The unit cost of V_{cmax} may be influenced by the costs of nitrogen uptake, which are likely higher (favouring investment in water transport) on less fertile soils. We tested for and detected a significant negative response of χ to soil pH, which indexes one dimension of soil fertility[29], accounting for an additional 5% of variance in χ. Predicted responses of the ratio J_{max}/V_{cmax} to temperature and CO_2 made with the simplifying assumption of a universally constant c^* appear to be supported by observational evidence, but should be analysed with a more extensive dataset.

This simple model's predictive skill suggests a route towards an improved predictive understanding and modelling approach for terrestrial carbon and water cycling while providing a new theoretical framework for the analysis of both environmental and plant morphological influences on photosynthetic traits. By making testable predictions of such influences based on quantifiable benefits and costs, the evolutionary optimality approach may lead to a more robust basis for understanding and modelling both the co-ordination of plant traits among species, and biological controls of the emergent functional properties of ecosystems as represented in ESMs.

Full Methods and any associated references are available in the online version of the paper.

Author Information Correspondence and requests for materials should be addressed to H.W. and C.P. (wanghan_sci@yahoo.com, peng.changhui@uqam.ca)

Acknowledgements

We thank Yan-Shih Lin, Vincent Maire, Belinda Medlyn, Beni Stocker, and IIASA colleagues for discussions, and Ralph Keeling for comments on successive drafts. The paper is a contribution to the AXA Chair Programme on Biosphere and Climate Impacts and Imperial College's initiative on Grand Challenges in Ecosystems and the Environment. Research is supported by National Basic Research

Programme of China (2013CB956602) grant to CP and HW, National Natural Science Foundation of China (Grant no. 31600388) to HW, an Australian Research Council Discovery grant ('Next-generation vegetation model based on functional traits') to ICP and IJW, an Australian National Data Service (ANDS) grant ('Ecosystem production in space and time') to ICP, and Terrestrial Ecosystem Research Council (TERN) grants ('Ecosystem Modelling and Scaling Infrastructure') to ICP and BJE. TERN and ANDS are supported by the Australian Government National Collaborative Infrastructure Strategy (NCRIS). TFK acknowledges financial support from the Laboratory Directed Research and Development (LDRD) fund under the auspices of DOE, BER Office of Science at Lawrence Berkeley National Laboratory, and a Macquarie University Research Fellowship. In addition to authors of this paper, data were provided by Margaret Barbour, Lucas Cernusak, Todd Dawson, David Ellsworth, Graham Farquhar, Howard Griffiths, Claudia Keitel, Alexander Knohl, Peter Reich, Dave Williams, Radika Bhaskar, Hans Cornelissen, Anna Richards, Susanne Schmidt, Fernando Valladares, Christian Körner, Ernst-Detlef Schulze, Nina Buchmann and Lou Santiago. We used 'free and fair use' eddy-covariance data acquired by the FLUXNET community and, in particular, by the following networks: AmeriFlux (US Department of Energy, Biological and Environmental Research, Terrestrial Carbon Program), AsiaFlux, CarboEuropeIP, Fluxnet-Canada (supported by CFCAS, NSERC, BIOCAP, Environment Canada, and NRCan), OzFlux and TCOS-Siberia. We acknowledge the financial support to the eddy-covariance data harmonization provided by CarboEuropeIP, FAO- GTOS-TCO, iLEAPS, Max Planck Institute for Biogeochemistry, National Science Foundation, University of Tuscia, Université Laval and Environment Canada and US Department of Energy and the database development and technical support from Berkeley Water Center, Lawrence Berkeley National Laboratory, Microsoft Research eScience, Oak Ridge National Laboratory, University of California–Berkeley, University of Virginia.

Author contributions

H.W. and I.C.P. derived the predictions. H.W. carried out all the analyses and constructed the Figures and Tables. I.C.P. and T.F.K contributed to the analysis and writing. T.W.D., B.J.E. and I.C.P. developed and tested the flux partitioning method. T.W.D. developed the global flux database and all the GPP computations. I.J.W. proposed least-cost hypothesis and contributed to the analysis. W.K.C. originated and compiled the $\Delta^{13}C$ data set. H.W. and I.C.P. wrote the first draft, and all authors contributed to the final draft.

Competing financial interests The authors declare no competing financial interests.

References

1 Ciais, P. *et al.* Carbon and other biogeochemical cycles. in Climate change 2013: the physical science basis. Contribution of Working Group I to the Fifth Assessment Report of the Intergovernmental Panel on Climate Change (eds Thomas F Stocker *et al.*) Ch. 6, 465-570 (Cambridge University Press, 2014).

2 Friedlingstein, P. *et al.* Uncertainties in CMIP5 climate projections due to carbon cycle feedbacks. *Journal of Climate* **27**, 511-526 (2014).

3 Prentice, I. C., Liang, X., Medlyn, B. E. & Wang, Y. P. Reliable, robust and realistic: the three R's of next-generation land-surface modelling. *Atmospheric Chemistry and Physics* **15**, 5987-6005 (2015).

4 Wang, H., Prentice, I. C. & Davis, T. W. Biophsyical constraints on gross primary production by the terrestrial biosphere. *Biogeosciences* **11**, 5987-6001 (2014).

5 Prentice, I. C., Dong, N., Gleason, S. M., Maire, V. & Wright, I. J. Balancing the costs of carbon gain and water transport: testing a new theoretical framework for plant functional ecology. *Ecology letters* **17**, 82-91 (2014).

6 Wright, I. J., Reich, P. B. & Westoby, M. Least‐Cost Input Mixtures of Water and Nitrogen for Photosynthesis. *The American Naturalist* **161**, 98-111 (2003).

7 Monteith, J. L. Solar radiation and productivity in tropical ecosystems. *Journal of Applied Ecology* **9**, 747-766 (1972).

8 Farquhar, G. D., von Caemmerer, S. & Berry, J. A. A biochemical model of photosynthetic CO_2 assimilation in leaves of C_3 species. *Planta* **149**, 78-90 (1980).

9 Medlyn, B. E. Physiological basis of the light use efficiency model. *Tree Physiology* **18**, 167-176 (1998).

10 Ali, A. *et al.* A global scale mechanistic model of the photosynthetic capacity. *Geoscientific Model Development Discussions* **8**, 6217–6266 (2015).

11 Cai, W. *et al.* Large differences in terrestrial vegetation production derived from satellite-based light use efficiency models. *Remote Sensing* **6**, 8945-8965 (2014).

12 De Kauwe, M. G. *et al.* Forest water use and water use efficiency at elevated CO2: a model‐data intercomparison at two contrasting temperate forest FACE sites. *Global Change Biology* **19**, 1759-1779 (2013).

13 Medlyn, B. E. *et al.* Reconciling the optimal and empirical approaches to modelling stomatal conductance. *Global Change Biology* **17**, 2134-2144 (2011).

14 Diefendorf, A. F., Mueller, K. E., Wing, S. L., Koch, P. L. & Freeman, K. H. Global patterns in leaf 13C discrimination and implications for studies of past and future climate. *Proceedings of the National Academy of Sciences* **107**, 5738-5743 (2010).

15 Cowan, I. & Farquhar, G. Stomatal function in relation to leaf metabolism and environment. *Symposia of the Society for Experimental Biology*, 471-505 (1977).

16 Givnish, T. J. *On the Economy of Plant Form and Function*. Vol. 6 (Cambridge University Press, 1986).

17 Cornwell, W. K. *et al.* A global dataset of leaf Δ13C values. doi:10.5281/zenodo.569501 (2017).

18 Farquhar, G. D., Ehleringer, J. R. & Hubick, K. T. Carbon isotope discrimination and photosynthesis. *Annual review of plant biology* **40**, 503-537 (1989).

19 Körner, C., Farquhar, G. & Wong, S. Carbon isotope discrimination by plants follows latitudinal and altitudinal trends. *Oecologia* **88**, 30-40 (1991).

20 Lin, Y.-S. *et al.* Optimal stomatal behaviour around the world. *Nature Climate Change* **5**, 459–464 (2015).

21 Maire, V. *et al.* The coordination of leaf photosynthesis links C and N fluxes in C3 plant species. *PloS one* **7**, e38345 (2012).

22 Haxeltine, A. & Prentice, I. C. A general model for the light-use efficiency of primary production. *Funct. Ecol.* **10**, 551-561, doi:10.2307/2390165 (1996).

23 Kattge, J. & Knorr, W. Temperature acclimation in a biochemical model of photosynthesis: a reanalysis of data from 36 species. *Plant, cell & environment* **30**, 1176-1190 (2007).

24 Collatz, G., Berry, J., Farquhar, G. & Pierce, J. The relationship between the Rubisco reaction mechanism and models of photosynthesis. *Plant, Cell & Environment* **13**, 219-225 (1990).

25 Beer, C. *et al.* Terrestrial gross carbon dioxide uptake: global distribution and covariation with climate. *Science* **329**, 834-838 (2010).

26 Yuan, W. *et al.* Global comparison of light use efficiency models for simulating terrestrial vegetation gross primary production based on the LaThuile database. *Agricultural and forest meteorology* **192**, 108-120 (2014).

27 Ainsworth, E. A. & Long, S. P. What have we learned from 15 years of free‐air CO_2 enrichment (FACE)? A meta‐analytic review of the responses of photosynthesis, canopy properties and plant production to rising CO_2. *New Phytologist* **165**, 351-372 (2005).

28 Frank, D. C. *et al.* Water-use efficiency and transpiration across European forests during the Anthropocene. *Nature Climate Change* **5**, 579-583 (2015).

29 Maire, V. *et al.* Global effects of soil and climate on leaf photosynthetic traits and rates. *Global Ecology and Biogeography* **24**, 706-717 (2015).

30 Kaplan, J. O. Geophysical applications of vegetation modeling. (Lund University, 2001).

Table 1 | Summary statistics for the environmental dependencies of χ (the ratio of leaf-internal to ambient CO_2 partial pressure). Logit-transformed values of χ derived from the global leaf stable carbon isotope dataset using a standard method[18] were regressed against the difference between growing-season mean temperature T_g and 25˚C (ΔT_g, ˚C), the natural logarithm of growing-season mean vapour pressure deficit at standard atmospheric pressure (ln D_0, kPa), and elevation (z, km). Theoretical values, shown for comparison, are partial derivatives of logit-transformed predicted 'optimal' χ with respect to each predictor, evaluated for standard conditions (T_g = 25 ˚C, D_0 = 1 kPa, z = 0 km).

Predictor	Theoretical value	Fitted coefficient	Confidence intervals		Multiple R^2
			2.5%	97.5%	
ΔT_g	**0.0545**	0.0515	0.0456	0.0575	0.391
ln D_0	**−0.5**	−0.5478	−0.6111	−0.4846	
z	**−0.0815**	−0.1065	−0.1315	−0.0815	
intercept	**1.189**	1.1680	1.0464	1.2896	

Figure 1 | Partial residual plots from the regression of logit-tranformed values of χ (the ratio of leaf-internal to ambient CO_2 partial pressure) derived from the global leaf stable carbon isotope dataset against environmental predictors. T_g: growing-season mean temperature. ln D_0: the natural logarithm of growing-season mean vapour pressure deficit at standard atmospheric pressure. z: elevation. Inset shows elevation responses for relative humidity (RH, %) classes with error bars showing 95% confidence intervals, compared to predicted responses (black dots) evaluated at the centre of each RH class.

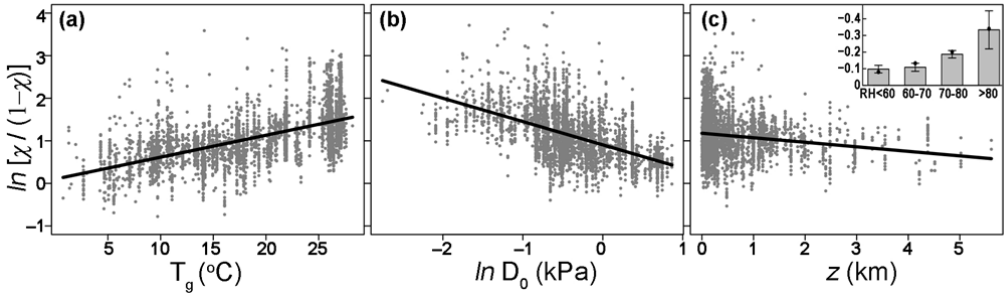

Figure 2 | Site-mean values of the ratio of leaf-internal to ambient CO_2 partial pressure (χ). Predictions (χ_o) are from the theoretical model driven by three environmental predictors (equation 1). Observations (χ) are from the global leaf stable carbon isotope dataset. Mean and standard deviation are shown for each biome. Biome types were assigned based on BIOME4[30] for consistency except for 'wetland' and 'alpine' types, which were assigned from source publications. The solid line is the regression through the origin; the dashed line is the 1:1 line. *r*: Pearson correlation between observed and predicted values; RMSE: root-mean-squared error of prediction.

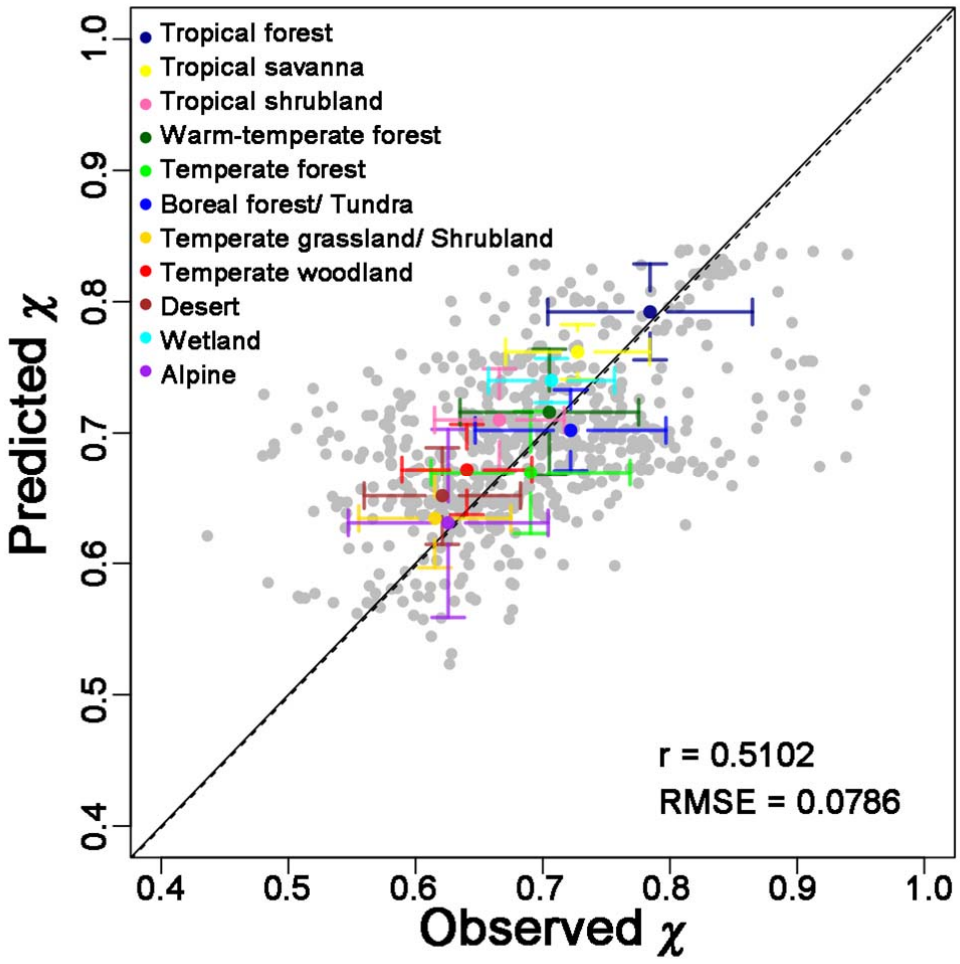

Figure 3 | Monthly gross primary production (GPP) at flux sites. Predictions from equations (2) and (3); observations based on CO_2 flux data in the FLUXNET archive. The solid line is the regression through the origin; the dashed line is the 1:1 line. *r*: Pearson correlation between observed and predicted values; RMSE: root-mean-squared error of prediction.

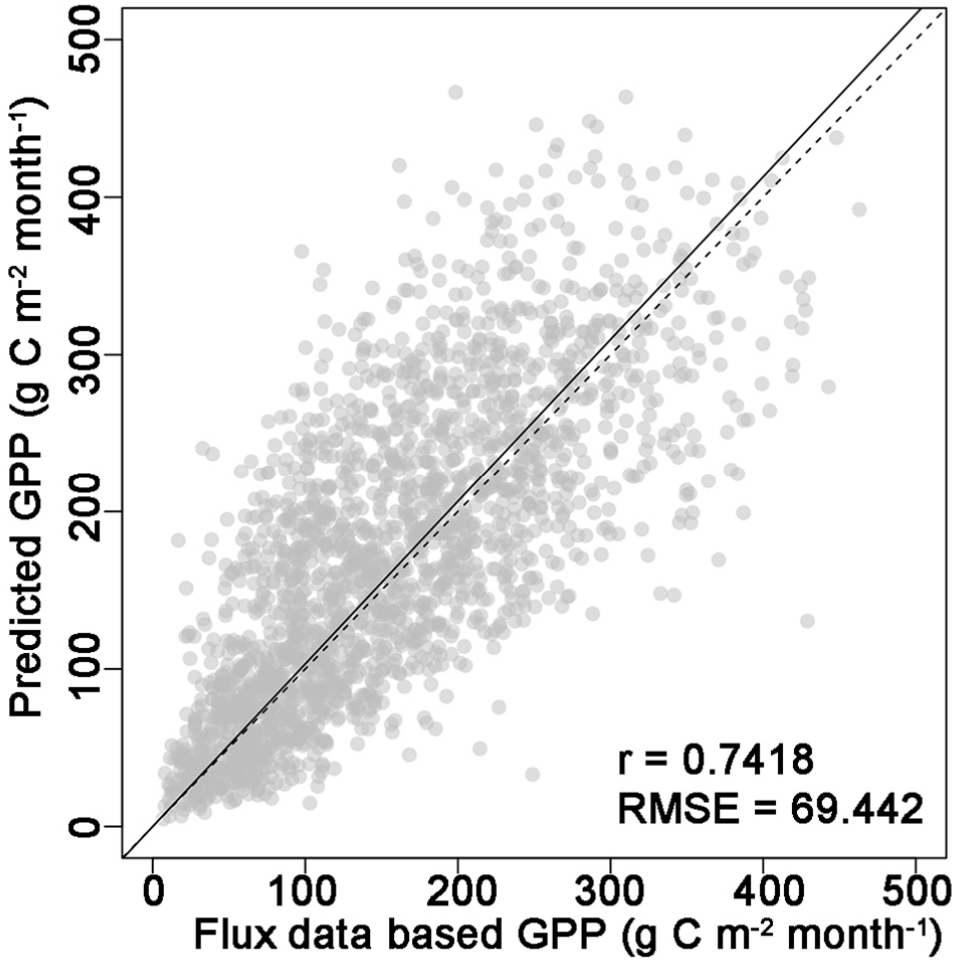

Methods

Theory for the environmental controls on χ

Optimality hypotheses to account for the environmental responses of stomata have a long history, with pioneering contributions especially by Cowan and Farquhar and Givnish[15,16]. Cowan and Farquhar hypothesized that stomata act to maximize marginal carbon gain (assimilation, A) while minimizing marginal water loss (transpiration, E), i.e. $\partial E / \partial A = \lambda$ where λ is a parameter representing the 'marginal carbon cost of water'. This approach successfully addresses many observed features of stomatal behaviour but leaves the value of λ undefined and, as noted by Givnish, does not explicitly consider the costs of maintaining photosynthetic capacity. These limitations are avoided by the *least-cost hypothesis*, which states that plants should minimize the combined carbon costs (per unit of assimilation) of maintaining the required capacities for carboxylation and transpiration. This hypothesis was first proposed explicitly by Wright et al.[6], and applied in the context of the standard model of photosynthesis[8] by Prentice et al.[5] who defined the following optimality criterion for χ:

$$a.\partial(E/A)/\partial\chi + b.\partial(V_{cmax}/A)/\partial\chi = 0 \quad (4)$$

Here, a and b are dimensionless cost factors for E and V_{cmax} respectively.

The *coordination hypothesis* states that V_{cmax} of leaves at any level in the canopy acclimates spatially and temporally to the prevailing daytime incident PPFD (the absorbed photosynthetic photon flux density) in such a way as to be neither in excess (entailing additional, futile maintenance respiration), nor less than required for full exploitation of the available light[21,22,31]. In other words, under typical daytime conditions when most photosynthesis takes place, the Rubisco-limited photosynthetic rate is equal to electron-transport limited photosynthetic rate ($A=A_C=A_J$). Therefore, Rubisco-limited photosynthesis in the standard biochemical model[8] can be rewritten as a prediction of V_{cmax}/A:

$$V_{cmax}/A = (\chi c_a + K)/(\chi c_a - \Gamma^*), \quad (5)$$

Fick's law of diffusion applied to both H_2O and CO_2 allows prediction of E/A:

$$E/A = 1.6(D/c_a)/(1-\chi) \quad (6)$$

where D is vapour pressure deficit. Initially neglecting Γ^* for simplicity (i.e. assuming $\chi c_a >> \Gamma^*$), substituting equations (5) and (6) in (4) and taking derivatives, the optimal value of χ satisfies:

$$1.6(aD/c_a)/(1-\chi)^2 - bK/\chi^2 c_a = 0 \quad (7)$$

The solution to equation (7) provides the required optimal value (χ_o):

$$\chi_o = \xi/(\xi+\sqrt{D}), \text{ where } \xi = \sqrt{(bK/1.6a)} \quad (8)$$

Omitting the assumption $\chi c_a >> \Gamma^*$ yields the more exact form:

$$\chi_o = \Gamma^*/c_a + (1 - \Gamma^*/c_a)\, \xi/(\xi+\sqrt{D}), \text{ where } \xi = \sqrt{[b(K+\Gamma^*)/1.6a]} \quad (9)$$

The parameter ξ expresses the sensitivity of χ_o to D. The ratio of stem respiration to transpiration capacity (a) depends (among other things) on the viscosity of water. The ratio of mitochondrial respiration to carboxylation capacity (b) is generally taken as constant[8]. As only the ratio b/a (not the individual terms b and a) affects χ_o, we will later use the composite parameter β to denote the value of b/a at 25˚C.

Given the particular form of equation (8), logit transformation simplifies the derivation of its sensitivities to environmental variables, as follows:

$$\text{logit}\,(\chi_o) = \ln [\chi_o/(1 - \chi_o)] = \tfrac{1}{2} \ln b - \tfrac{1}{2} \ln a + \tfrac{1}{2} \ln K - \tfrac{1}{2} \ln D - \tfrac{1}{2} \ln 1.6 \quad (10)$$

The dependencies of a (through the viscosity of water η) and K (through the Michaelis-Menten coefficients of Rubisco for carboxylation (K_c) and oxygenation (K_o)) on temperature (T), and the dependency of K (through P_o, the partial pressure of O_2) and D on elevation, are denoted by $f_1(T)$, $f_2(T)$, $g_1(z)$ and $g_2(z)$. The elevation effect here includes the effect of the vapour pressure decline because humidity statistics in the 3D-gridded datasets used for global analysis do not account for it. Thus, we substitute D with D_0 (the vpd that would be obtained at standard atmospheric pressure under the same temperature and H_2O mole fraction). Equation (10) is then equivalent to:

$$\ln [\chi_o/(1 - \chi_o)] = -\tfrac{1}{2} \ln f_1(T) + \tfrac{1}{2} \ln f_2(T) + \tfrac{1}{2} \ln g_1(z) - \tfrac{1}{2} \ln D_0 - \tfrac{1}{2} \ln g_2(z) + C, \quad (11)$$

$$\text{where } C = \tfrac{1}{2} (\ln b - \ln a_{ref} + \ln K_{ref} - \ln 1.6) = \tfrac{1}{2} (\ln \beta + \ln K_{ref} - \ln 1.6) \quad (12)$$

a_{ref} and K_{ref} are the values of a and K under standard conditions (T = 298 K, z = 0). Equation (11) predicts the coefficient of $\ln D_0$ as –0.5.

Temperature dependency of a

The parameter a is directly proportional to η, according to equation (11) in ref. 5. The temperature dependency of η can be well approximated by the Vogel equation[32]:

$$\eta = 10^{-3} \exp [A + B/(C + T)] \quad (13)$$

where A = –3.719, B = 580 and C = –138. Thus, the sensitivity of η to temperature is given by:

$$(1/\eta)\, \partial\eta/\partial T = \partial \ln \eta/\partial T = -B/(C + T)^2 \quad (14)$$

allowing the response of η to T, within the physiologically relevant range, to be well approximated by an exponential response to $\Delta T = T - 298$ K relative to a reference value at T = 298 K (η_{ref}):

$$f_1(T) = \eta/\eta_{ref} \approx \exp [-B/(C + T)^2\, \Delta T\,] \quad (15)$$

Temperature and elevation dependencies of K

K (in partial pressure units) is given by:

$$K = K_c (1 + P_o/K_o), \quad (16)$$

P_o can be expressed as a simple function of elevation (in km) using a standard approximation for the decline in atmospheric pressure with elevation[33]:

$$P_o = 21000 \exp(-0.114\, z) \quad (17)$$

The Arrhenius relationship describing the response of a biochemical rate parameter (x, such as K_c and K_o) to temperature can be expressed as:

$$\partial \ln x/\partial T = (\Delta H/R).(1/T^2) \quad (18)$$

where R = 8.3145 J mol^{-1} K^{-1} and the activation energies ΔH are 79.43 kJ mol^{-1} for K_c and 36.38 kJ mol^{-1} for K_o, denoted as ΔH_c and ΔH_o, respectively, from *in vivo* determinations[34].

Therefore, the sensitivity of K to temperature from equation (16) is given by:

$$(1/K)\, \partial K/\partial T = [(\Delta H_c/R)(1/T^2)\,(P_o + K_o) - (\Delta H_o/R)(1/T^2)\, P_o]/(P_o + K_o) \quad (19)$$

leading to:

$$f_2(T) = \exp([(\Delta H_c/R)(1/T^2)\,(P_o + K_o) - (\Delta H_o/R)(1/T^2)\, P_o]/(P_o + K_o)\, \Delta T) \quad (20)$$

The sensitivity of K to elevation due to declination in P_o can then be derived from equation (16):

$$(1/K)\, \partial K/\partial z = -0.114\, P_o/(P_o + K_o) \quad (21)$$

Therefore,

$$g_1(z) = \exp[-0.114\, P_o/(P_o + K_o) z] \quad (22)$$

Elevation dependency of D

D can similarly be expressed as a function of elevation:

$$D = e_s - e_{a0} \exp(-0.114\, z) \quad (23)$$

where e_s is the saturation vapour pressure and e_{a0} is the actual vapour pressure that would be obtained at sea level under the same H_2O mole fraction and temperature. Since exp (–0.114z) can be taken as equal to unity, to a good approximation, within the relevant range of z, the dependency of D on elevation here approximated as:

$$\partial \ln D/\partial z = 0.114\, e_{a0}/D_0 = 0.114\, RH/(1 - RH), \quad (24)$$

Therefore,

$$g_2(z) = \exp\{0.114\,[RH/(1 - RH)]\, z\} \quad (25)$$

Note that this theoretically derived elevation effect on D varies strongly with RH, approaching infinity as RH tends to 1.

Linearized expressions for χ_o in terms of environmental predictors

Evaluating equations (15), (20), (22) and (25) at standard temperature (T = 298 K, z = 0 and RH_0 = 50%) and substituting the resulting expressions in equation (11), we obtain:

$$\ln[\chi_o/(1 - \chi_o)] = \tfrac{1}{2}(0.0864 + 0.0227)\,\Delta T - \tfrac{1}{2}(0.0491 + 0.114)\, z - \tfrac{1}{2}\ln D_0 + C$$

$$= 0.0545\,\Delta T - 0.0815\, z - 0.5 \ln D_0 + C \quad (26)$$

$C \approx 1.189$, estimated as the intercept in a generalized linear model (GLM) fitted to the data with imposed regression coefficients for all three environmental effects in equation (26). This allows us to estimate $\beta \approx 240$ from equation (12). Therefore, the optimal leaf-internal partial pressure of CO_2 can be derived from the more exact expression for χ_o (equation 9):

$$c_i = \frac{\xi c_a + \Gamma^*\sqrt{D}}{\xi + \sqrt{D}},\ \xi = \sqrt{\frac{\beta\left(K + \Gamma^*\right)}{1.6\eta^*}}, \quad (27)$$

Here η^* is the viscosity of water relative to its value at 25˚C, representing the effect of changing viscosity on the value of a.

Testing the theory with global $\delta^{13}C$ data

Vascular-plant leaf stable carbon isotope data were compiled from published and unpublished sources[17]. Inferred carbon isotope discrimination (Δ) values for 3549 leaf samples of C_3 plants were converted to estimates of χ by a standard equation[18]:

$$\chi = \frac{\Delta - a'}{b' - a'} \quad (28)$$

where a' and b' have standard values 4.4 and 27, representing the diffusional and biochemical components of carbon isotope discrimination, respectively. The Climatic Research Unit CL2.0 10-minute gridded monthly climatology[35] of mean, maximum and minimum temperatures and relative humidity provided mean temperature (T_g, ˚C) and vapour pressure deficit (D_0, kPa) values for the period with daily mean temperatures > 0˚C. Values of $\ln[\chi/(1-\chi)]$ were fitted using a GLM with $\Delta T_g = T_g - 25$˚C, $\ln D_0$, and site-specific elevation (z, km) as predictors. Standard errors estimated by the

GLM were combined quadratically with standard errors for the uncertainty of the effective Rubisco discrimination parameter b', the latter obtained by generating 10^4 normally distributed values of b' (mean = 27, standard deviation = 0.27) and repeating the estimation of χ and the GLM fitting 10^4 times with different b' values.

Incorporating finite g_m into the least-cost framework and testing with global $\delta^{13}C$ data

Mesophyll conductance, the liquid-phase conductance between the intercellular spaces and the chloroplasts, is assumed arbitrarily large in most large-scale ecophysiological data analysis and models[36], since the mechanisms behind its environmental responses remain unclear. The prediction of g_m still largely relies on empirical relationships[37]. However, the effect of finite g_m can be incorporated into the least-cost framework naturally due to its impact on carboxylation, and furthermore leads to an optimal ratio of the chloroplastic to ambient CO_2 (χ_c) under the simplifying assumption that the ratio of g_s (stomata conductance) to g_m is independent of environmental factors[38-41].

Assuming that the total conductance (g) for CO_2 diffusing from the ambient atmosphere to the chloroplasts is principally controlled by g_s and g_m:

$$1/g = 1/g_s + 1/g_m \tag{29}$$

Note that g_m affects CO_2 diffusion for carboxylation, but not H_2O diffusion during transpiration. Replacing stomatal with total conductance for carboxylation, equation (6) therefore becomes:

$$E/A = 1.6\,(D/c_a)\,(g_s + g_m) / [(1-\chi_c)\,g_m] \tag{30}$$

The leaf-internal CO_2 concentration (χc_a) in equation (5) can then be replaced by the chloroplastic CO_2 concentration ($\chi_c c_a$):

$$V_{cmax}/A = (\chi_c c_a + K)/(\chi_c c_a - \Gamma^*) \tag{31}$$

Applying the optimality criterion:

$$a.\partial(E/A_c)/\partial\chi_c + b.\partial(V_{cmax}/A_c)/\partial\chi_c = 0 \tag{32}$$

to equations (30) and (31), the optimal ratio of chloroplast to ambient CO_2 (χ_{co}) is given by (assuming $\chi_c c_a >> \Gamma^*$):

$$\chi_{co} = \xi_c/(\xi_c+\sqrt{D}), \text{ where } \xi_c = \sqrt{[bK/1.6a/(1+ g_s/g_m)]} = \xi / \sqrt{(1+ g_s/g_m)}, \tag{33}$$

or, if we relax the assumption $\chi_c c_a >> \Gamma^*$, by:

$$\chi_{co} = \Gamma^*/c_a + (1-\Gamma^*/c_a)\,\xi_c/(\xi_c+\sqrt{D}), \text{ where } \xi_c = \sqrt{\{b(K+\Gamma^*)/[1.6a(1+ g_s/g_m)]\}} \tag{34}$$

Here χ_{co} is not influenced by g_s and g_m separately, but by their ratio. The form of the model for χ_{co} resembles that for χ_o, but the sensitivity parameter ξ is adjusted by a factor $\sqrt{[1/(1+ g_s/g_m)]}$.

In the model for χ_{co} the ratio of g_s to g_m is assumed to be independent of environment. Even though both g_s and g_m vary with environmental conditions, including light, moisture and temperature, their covariation under a wide range of conditions supports this assumption at least as a first approximation[38-41]. Moreover, data indicate that the value of g_s/g_m is quite conservative, with a median of about 1.4 (I.J. Wright, unublished data). The derivation of the environmental dependencies of χ_{co} then follows the same logical steps as that for χ. Further refinement of the model for χ_{co} however would require deeper understanding of the regulation of g_s and g_m.

The estimated value of the ratio of cost factors b to a at reference temperature is updated to a value of 343 after deducting the term of $(g_s/g_m + 1)^{-1}$ from constant C. This time we obtained C based on observational χ_c estimated from the global carbon isotope dataset with the "comprehensive" equation in Ubierna & Farquhar[42] but following the first three simplifying assumptions listed in their Figure 1: (1) that the ternary effect is negligible; (2) the fractionations associated with Rubisco carboxylation, during respiration and photorespiration are far less than 1; (3) infinite boundary-layer conductance. We also assumed leaf dark respiration $R_d << A$, so that $R_d/(R_d + \mathrm{A}) \approx R_d/A$. The "comprehensive" equation for Δ can then be rewritten more simply as:

$$\Delta = a_s (1 - \chi) + a_m (\chi - \chi_c) + b\chi_c - eb_0 (\chi_c + \kappa) - f\gamma \quad (35)$$

Here, a_s, a_m, b, e and f are the fractionations associated with diffusion in air (4.4‰), in water (1.8‰), by Rubisco carboxylation (27 to 30‰), during respiration (0 to –5‰) and photorespiration (8 to 16‰), respectively. $b_0 = R_d/V_{cmax} = 0.015$[8] , $\kappa = K/c_a$ and $\gamma = \Gamma^*/c_a$.

Given that the CO_2 flux from the outside to the intercellular spaces must be the same as that from the intercellular spaces to the chloroplast, denoting the ratio of g_m to g_s as θ, we have:

$$(1 - \chi)\, g_s = (\chi - \chi_c)\, \theta\, g_s \quad (36)$$

Therefore:

$$1 - \chi = \theta\, (1 - \chi_c)/(1 + \theta) \quad (37)$$

and

$$\chi - \chi_c = (1 - \chi_c)/(1 + \theta) \quad (38)$$

Substituting these expressions into equation (35) and solving for χ_c gives:

$$\chi_c = \frac{\Delta - \dfrac{\theta a_s + a_m}{1+\theta} + eb_0\kappa + f\gamma}{b - \dfrac{\theta a_s + a_m}{1+\theta} - eb_0} \quad (39)$$

We assumed a constant value of θ = 1.4, based on data compiled by IJW, and consistent with values in the literature[43].

Given the uncertainties in parameters b, e and f, we chose the values (b = 30, e = 0, f = 16) that produced the best fit (R^2 = 0.5057) in the regression of χ_c against temperature, ln vpd and elevation (Supplementary Table 2).

Light-use efficiency model

The model proposed by Wang et al.[4] assumed that the electron-transport and Rubisco-limited rates of photosynthesis (A_J, A_c) as described by the biochemical photosynthesis model[8] are coordinated (that is, $A = A_J = A_c$) under typical daytime conditions[21,22,31], allowing GPP to be predicted from A_J at a monthly time scale by:

$$A_J = \varphi_0 I_{abs} (c_i - \Gamma^*)/(c_i + 2\Gamma^*) \quad (40)$$

LUE is the product of φ_0 and the CO_2 limitation term of $(c_i - \Gamma^*)/(c_i + 2\Gamma^*)$ (denoted here by m). Incorporating the exact equation for c_i (equation 27) yields:

$$A = \varphi_0 I_{abs} m \quad (41)$$

where

$$m = \frac{c_a - \Gamma^*}{c_a + 2\Gamma^* + 3\Gamma^* \sqrt{\frac{1.6 D \eta^*}{\beta\left(K + \Gamma^*\right)}}} \quad (42)$$

Equations (41) and (42) assume that the light response of A is linear up to the coordination point, i.e. that the maximum electron-transport rate (J_{max}) is arbitrarily large. In reality J_{max} limitation can be significant, especially at high temperatures. We therefore modified equation (41) to allow for a non-rectangular hyperbola relationship between A and I_{abs}[44,45]:

$$A = \varphi_0 I_{abs} m \frac{1}{\sqrt{1 + \left(\frac{4\varphi_0 I_{abs}}{J_{max}}\right)^2}} \quad (43)$$

This does not have the form of a LUE model, because of the non-linear dependence on I_{abs}. However, the apparent discrepancy between the non-linear light response observed at short time scales (sub-daily) and the linear light response described by the empirical LUE model on longer time scales (weekly to monthly) can be resolved if it is assumed J_{max} acclimates to I_{abs} over longer time scales. To show this, we further assume that (a) there exists an optimal J_{max} for given average light conditions that maximizes the differences between the benefit and cost of maintaining this value of J_{max}, which conceptually includes the maintenance of light-harvesting complexes and the various proteins involved in electron transport; (b) the benefit is the assimilation rate A, whereas the cost is the product of J_{max} and a parameter c (defined as the unit cost of maintaining J_{max}); (c) V_{cmax} and J_{max} vary with

environmental conditions on a monthly time scale, while the unit costs b and c of maintaining V_{cmax} and J_{max} respectively are unchanged; and (d) V_{cmax} and J_{max} are related via the coordination hypothesis ($A_c = A_J = A$). The optimality criterion for J_{max} is then simply:

$$\partial A/\partial J_{max} = c \tag{44}$$

Taking the partial derivative of A with respect to J_{max} in equation (43) leads to:

$$c = \frac{\partial A}{\partial J_{\max}} = \frac{m\left(\varphi_0 I_{abs}\right)^3}{4\sqrt{\left[\left(\varphi_0 I_{abs}\right)^2 + \left(\frac{J_{\max}}{4}\right)^2\right]^3}} \tag{45}$$

Equation (43) can now be rewritten as

$$A = \varphi_0 I_{abs} m \sqrt{1 - \left(\frac{4c}{m}\right)^{\frac{2}{3}}} \tag{46}$$

This is a key algebraic result because A is now, once again, proportional to I_{abs}.

Next, applying the coordination hypothesis ($A_c = A_J = A$):

$$\frac{\varphi_0 I_{abs}}{\sqrt{\left(\varphi_0 I_{abs}\right)^2 + \left(\frac{J_{\max}}{4}\right)^2}} = \frac{4V_{c\max}\left(c_i - \Gamma^*\right)}{J_{\max}\left(c_i + K\right)m} \tag{47}$$

Substituting equation (47) into equation (45) and expanding the CO_2 limitation term m, we can express equation (45) as:

$$c = \frac{\partial A}{\partial J_{\max}} = 16\left(c_i + 2\Gamma^*\right)^2\left(c_i - \Gamma^*\right)\left(\frac{V_{c\max}}{J_{\max}\left(c_i + K\right)}\right)^3 \tag{48}$$

Taking typical values of $J_{max}/V_{cmax} = 1.88$[23] and $\chi = 0.8$[46], we estimate $c = 0.103$ for standard conditions ($T = 25$ °C, $z = 0$ km, c_a=400 ppm), leading to:

$$A = \varphi_0 I_{abs} m \sqrt{1 - \left(\frac{c^*}{m}\right)^{\frac{2}{3}}} \tag{49}$$

where

$$m = \frac{c_a - \Gamma^*}{c_a + 2\Gamma^* + 3\Gamma^* \sqrt{\dfrac{1.6 D \eta^*}{\beta\left(K + \Gamma^*\right)}}} \quad (50)$$

and the constant c^* is 4 times c, the unit cost of maintaining J_{max}. As an indirect test of the assumptions, the responses of J_{max}/V_{cmax} to temperature and CO_2 from equation (48) are compared with observations (Supplementary Information).

A fuller derivation of χ, χ_c and light-use efficiency model is provided in Supplementary Information.

GPP data-model comparison

Equations (2)-(3) yielded modelled site-specific monthly GPP values for comparison with values independently derived from eddy-covariance measurements of CO_2 exchange in the Free and Fair Use subset of the FLUXNET archive, using a consistent gap-filling procedure (Supplementary Information). The monthly GPP data derived from flux measurements are archived in BitBucket (Data link: https://bitbucket.org/labprentice/gepisat/src/8d34456aafcd/results) for public access. For the modelled values, monthly LUE was estimated based on temperature and vapour pressure extracted from CRU time-series (TS 3.22) data at 0.5˚ resolution[47] and site-observed c_a. Monthly absorbed PPFD was estimated as the product of PPFD (0.45 times the WATCH incident surface shortwave radiation[48], divided by 0.22 J μmol^{-1}) and the MODIS Enhanced Vegetation Index (EVI), equated to the fraction of photosynthetically active radiation absorbed by foliage[49]. To match the WATCH data resolution, wherever each site was located, EVI was upscaled from to the 0.5˚ grid cell based on the arithmetic mean of the 100 valid 0.05º pixels within each pixel at the 0.5º resolution.

Data availability

The global carbon isotope dataset used here is available in GitHub with DOI: 10.5281/zenodo.569501[17].

References

1 Ciais, P. *et al.* Carbon and other biogeochemical cycles. in Climate change 2013: the physical science basis. Contribution of Working Group I to the Fifth Assessment Report of the Intergovernmental Panel on Climate Change (eds Thomas F Stocker *et al.*) Ch. 6, 465-570 (Cambridge University Press, 2014).

2 Friedlingstein, P. *et al.* Uncertainties in CMIP5 climate projections due to carbon cycle feedbacks. *Journal of Climate* **27**, 511-526 (2014).

3 Prentice, I. C., Liang, X., Medlyn, B. E. & Wang, Y. P. Reliable, robust and realistic: the three R's of next-generation land-surface modelling. *Atmospheric Chemistry and Physics* **15**, 5987-6005 (2015).

4 Wang, H., Prentice, I. C. & Davis, T. W. Biophsyical constraints on gross primary production by the terrestrial biosphere. *Biogeosciences* **11**, 5987-6001 (2014).

5 Prentice, I. C., Dong, N., Gleason, S. M., Maire, V. & Wright, I. J. Balancing the costs of carbon gain and water transport: testing a new theoretical framework for plant functional ecology. *Ecology letters* **17**, 82-91 (2014).

6 Wright, I. J., Reich, P. B. & Westoby, M. Least‐cost input mixtures of water and nitrogen for photosynthesis. *The American Naturalist* **161**, 98-111 (2003).

7 Monteith, J. L. Solar radiation and productivity in tropical ecosystems. *Journal of Applied Ecology* **9**, 747-766 (1972).

8 Farquhar, G. D., von Caemmerer, S. & Berry, J. A. A biochemical model of photosynthetic CO_2 assimilation in leaves of C_3 species. *Planta* **149**, 78-90 (1980).

9 Medlyn, B. E. Physiological basis of the light use efficiency model. *Tree Physiology* **18**, 167-176 (1998).

10 Ali, A. *et al.* A global scale mechanistic model of the photosynthetic capacity. *Geoscientific Model Development Discussions* **8**, 6217–6266 (2015).

11 Cai, W. *et al.* Large differences in terrestrial vegetation production derived from satellite-based light use efficiency models. *Remote Sensing* **6**, 8945-8965 (2014).

12 De Kauwe, M. G. *et al.* Forest water use and water use efficiency at elevated CO_2: a model‐data intercomparison at two contrasting temperate forest FACE sites. *Global Change Biology* **19**, 1759-1779 (2013).

13 Medlyn, B. E. *et al.* Reconciling the optimal and empirical approaches to modelling stomatal conductance. *Global Change Biology* **17**, 2134-2144 (2011).

14 Diefendorf, A. F., Mueller, K. E., Wing, S. L., Koch, P. L. & Freeman, K. H. Global patterns in leaf 13C discrimination and implications for studies of past and future climate. *Proceedings of the National Academy of Sciences* **107**, 5738-5743 (2010).

15 Cowan, I. & Farquhar, G. Stomatal function in relation to leaf metabolism and environment. *Symposia of the Society for Experimental Biology*, 471-505 (1977).

16 Givnish, T. J. *On the Economy of Plant Form and Function*. Vol. 6 (Cambridge University Press, 1986).

17 Cornwell, W. K. *et al.* A global dataset of leaf $\Delta^{13}C$ values. doi:10.5281/zenodo.569501 (2017).

18 Farquhar, G. D., Ehleringer, J. R. & Hubick, K. T. Carbon isotope discrimination and photosynthesis. *Annual review of plant biology* **40**, 503-537 (1989).

19 Körner, C., Farquhar, G. & Wong, S. Carbon isotope discrimination by plants follows latitudinal and altitudinal trends. *Oecologia* **88**, 30-40 (1991).

20 Lin, Y.-S. *et al.* Optimal stomatal behaviour around the world. *Nature Climate Change* **5**, 459–464 (2015).

21 Maire, V. *et al.* The coordination of leaf photosynthesis links C and N fluxes in C_3 plant species. *PloS one* **7**, e38345 (2012).

22 Haxeltine, A. & Prentice, I. C. A general model for the light-use efficiency of primary production. *Funct. Ecol.* **10**, 551-561, doi:10.2307/2390165 (1996).

23 Kattge, J. & Knorr, W. Temperature acclimation in a biochemical model of photosynthesis: a reanalysis of data from 36 species. *Plant, cell & environment* **30**, 1176-1190 (2007).

24 Collatz, G., Berry, J., Farquhar, G. & Pierce, J. The relationship between the Rubisco reaction mechanism and models of photosynthesis. *Plant, Cell & Environment* **13**, 219-225 (1990).

25 Beer, C. *et al.* Terrestrial gross carbon dioxide uptake: global distribution and covariation with climate. *Science* **329**, 834-838 (2010).

26 Yuan, W. *et al.* Global comparison of light use efficiency models for simulating terrestrial vegetation gross primary production based on the LaThuile database. *Agricultural and forest meteorology* **192**, 108-120 (2014).

27 Ainsworth, E. A. & Long, S. P. What have we learned from 15 years of free‐air CO_2 enrichment (FACE)? A meta‐analytic review of the responses of photosynthesis, canopy properties and plant production to rising CO_2. *New Phytologist* **165**, 351-372 (2005).

28 Frank, D. C. *et al.* Water-use efficiency and transpiration across European forests during the Anthropocene. *Nature Climate Change* **5**, 579-583 (2015).

29 Maire, V. *et al.* Global effects of soil and climate on leaf photosynthetic traits and rates. *Global Ecology and Biogeography* **24**, 706-717 (2015).

30 Kaplan, J. O. Geophysical applications of vegetation modeling. (Lund University, 2001).

31 Chen, J.-L., Reynolds, J. F., Harley, P. C. & Tenhunen, J. D. Coordination theory of leaf nitrogen distribution in a canopy. *Oecologia* **93**, 63-69 (1993).

32 Vogel, H. Temperaturabhängigkeitsgesetz der Viskosität von Flüssigkeiten. *Physik Z* **22**, 645-646 (1921).

33 Jacob, D. *Introduction to atmospheric chemistry*. (Princeton University Press, 1999).

34 Bernacchi, C. J., Singsaas, E. L., Pimentel, C., Portis Jr, A. R. & Long, S. P. Improved temperature response functions for models of Rubisco‐limited photosynthesis. *Plant, Cell & Environment* **24**, 253-259 (2001).

35 New, M., Lister, D., Hulme, M. & Makin, I. A high-resolution data set of surface climate over global land areas. *Climate research* **21**, 1-25 (2002).

36 Keenan, T. F., Sabate, S. & Gracia, C. Soil water stress and coupled photosynthesis–conductance models: Bridging the gap between conflicting reports on the relative roles of stomatal, mesophyll conductance and biochemical limitations to photosynthesis. *Agricultural and Forest Meteorology* **150**, 443-453 (2010).

37 Sun, Y. *et al.* Impact of mesophyll diffusion on estimated global land CO_2 fertilization. *Proceedings of the National Academy of Sciences* **111**, 15774-15779 (2014).

38 Flexas, J., Ribas‐Carbo, M., DIAZ‐ESPEJO, A., GalmES, J. & Medrano, H. Mesophyll conductance to CO_2: current knowledge and future prospects. *Plant, Cell & Environment* **31**, 602-621 (2008).

39 Gu, J., Yin, X., Stomph, T.-J., Wang, H. & Struik, P. C. Physiological basis of genetic variation in leaf photosynthesis among rice (Oryza sativa L.) introgression lines under drought and well-watered conditions. *Journal of experimental botany* **63**, 5137-5153 (2012).

40 Douthe, C., Dreyer, E., Epron, D. & Warren, C. Mesophyll conductance to CO_2, assessed from online TDL-AS records of $^{13}CO_2$ discrimination, displays small but significant short-term responses to CO_2 and irradiance in *Eucalyptus* seedlings. *Journal of Experimental Botany* **62**, 5335-5346 (2011).

41 Barbour, M., Warren, C., Farquhar, G., Forrester, G. & Brown, H. Variability in mesophyll conductance between barley genotypes, and effects on transpiration efficiency and carbon isotope discrimination. *Plant, Cell & Environment* **33** (2010).

42 Ubierna, N. & Farquhar, G. D. Advances in measurements and models of photosynthetic carbon isotope discrimination in C_3 plants. *Plant, cell & environment* **37**, 1494-1498 (2014).

43 Warren, C. R. Stand aside stomata, another actor deserves centre stage: the forgotten role of the internal conductance to CO_2 transfer. *Journal of Experimental Botany* **59**, 1475-1487 (2008).

44 Smith, E. L. The influence of light and carbon dioxide on photosynthesis. *The Journal of general physiology* **20**, 807-830 (1937).

45 Harley, P. C., Thomas, R. B., Reynolds, J. F. & Strain, B. R. Modelling photosynthesis of cotton grown in elevated CO_2. *Plant, Cell & Environment* **15**, 271-282 (1992).

46 Lloyd, J. & Farquhar, G. D. ^{13}C discrimination during CO_2 assimilation by the terrestrial biosphere. *Oecologia* **99**, 201-215 (1994).

47 Harris, I., Jones, P., Osborn, T. & Lister, D. Updated high-resolution grids of monthly climatic observations–the CRU TS3.10 Dataset. *International Journal of Climatology* **34**, 623-642 (2014).

48 Weedon, G. P. *et al.* The WFDEI meteorological forcing data set: WATCH Forcing Data methodology applied to ERA-Interim reanalysis data. *Water Resources Research* **50**, 7505-7514 (2014).

49 Xiao, X., Zhang, Q., Hollinger, D., Aber, J. & Moore, B. I. Modeling gross primary production of an evergreen needleleaf forest using MODIS and climate data. *Ecol. Appl.* **15**, 954-969 (2005).

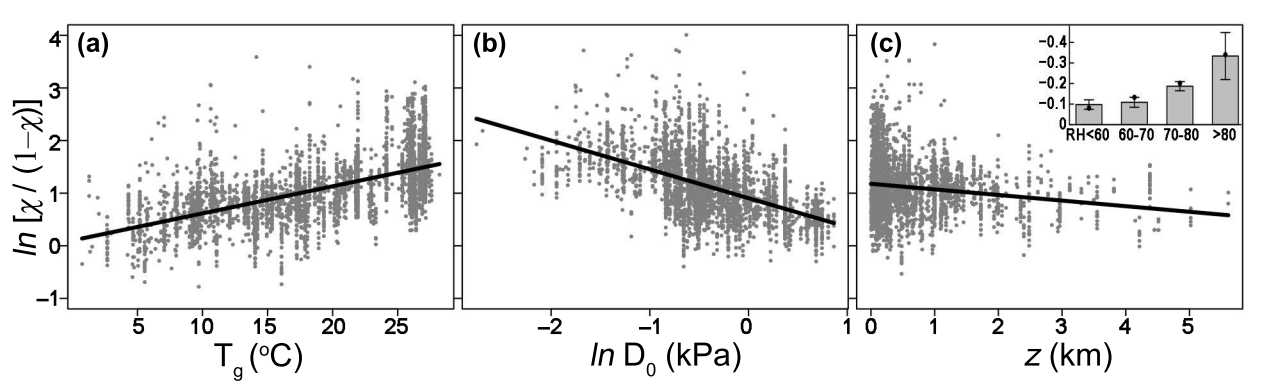
(a)
(b)
(c)
ln [χ / (1−χ)]
T_g (°C)
ln D_0 (kPa)
z (km)
RH<60
60-70
70-80
>80

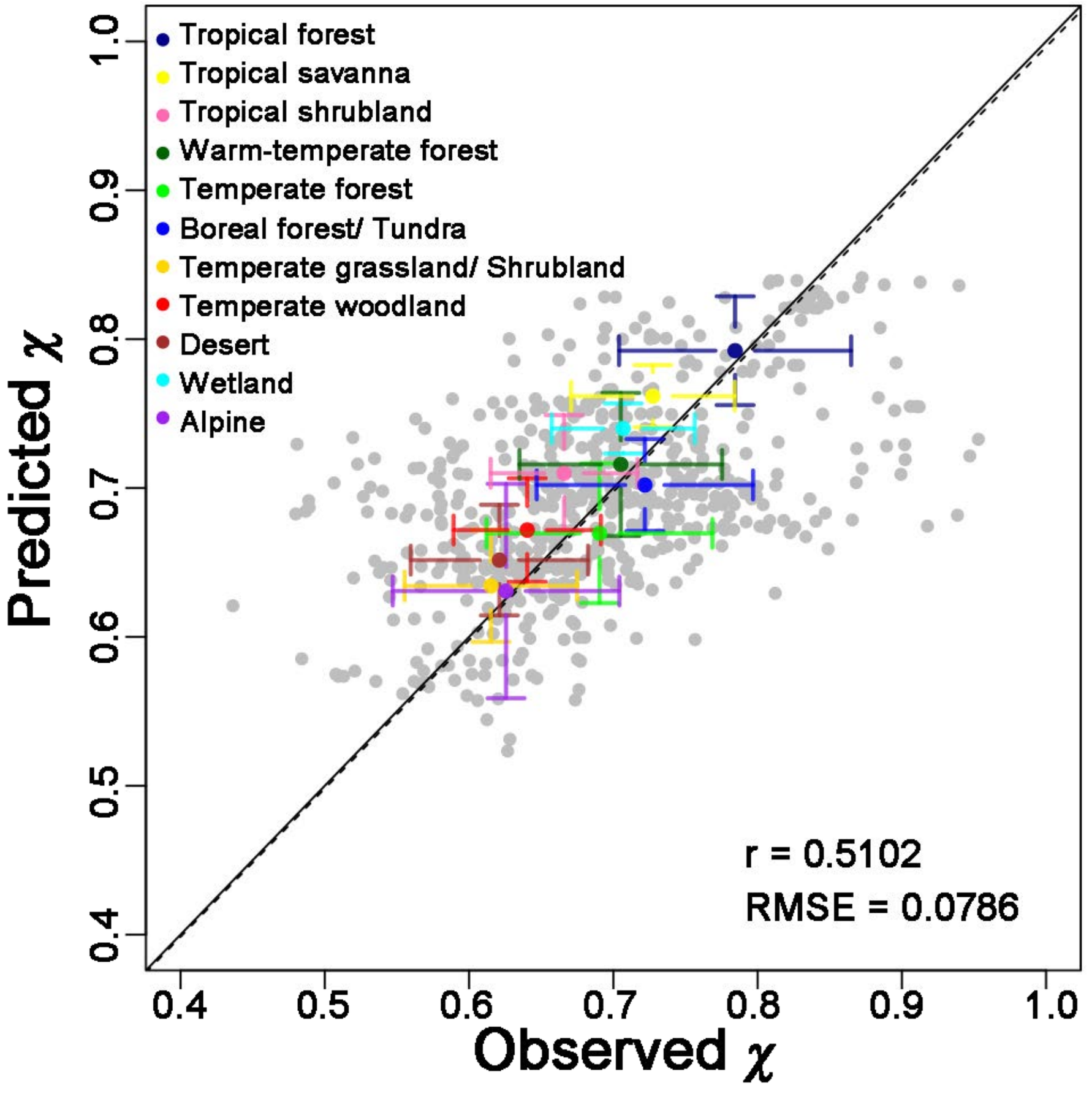
Tropical forest
Tropical savanna
Tropical shrubland
Warm-temperate forest
Temperate forest
Boreal forest/ Tundra
Temperate grassland/ Shrubland
Temperate woodland
Desert
Wetland
Alpine
r = 0.5102
RMSE = 0.0786
Predicted χ
Observed χ
0.4
0.5
0.6
0.7
0.8
0.9
1.0

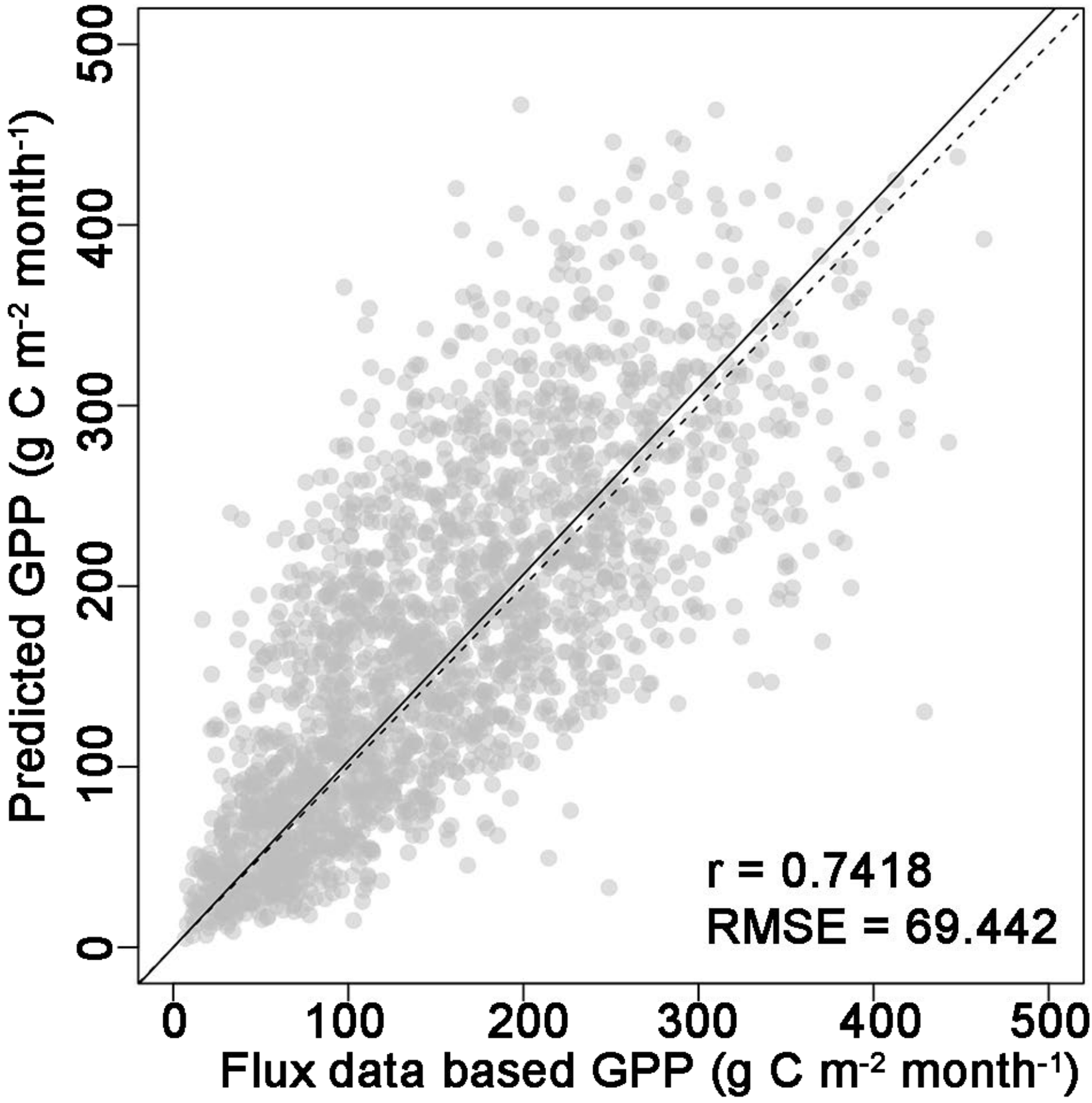
Predicted GPP (g C m-2 month-1)
0
100
200
300
400
500
Flux data based GPP (g C m-2 month-1)
0
100
200
300
400
500
r = 0.7418
RMSE = 69.442